Multi-mode Cepheids in the Large Magellanic Cloud - Challenges for Theory

W. A. Dziembowski and R. Smolec
Warsaw University Observatory and Nicolaus Copernicus Astronomical Center, Warsaw, Poland

Data from the OGLE-III Catalog

The OGLE-III catalog of the LMC Cepheids (Soszyński et al. 2008b) contains a large number of objects with more than one mode excited. There are 61 classical beat Cepheids pulsating in the fundamental and first overtone modes (**F/1O**) and 203 objects pulsating in the first two overtones (**1O/2O**). The rare types of multimode radial pulsators (Soszyński et al. 2008a) include two **1O/3O** objects, two triple-mode pulsators of the **F/1O/2O** type and three of the **1O/2O/3O** type. Of these rare Cepheids, only two 1O/2O/3O objects were known before (Moskalik et al. 2004). **Figures 1 and 2** show data (Petersen and PL diagrams) for the F/1O and 1O/2O Cepheids, respectively. In these figures, data for the triple-mode objects are also depicted.

In a number of LMC Cepheids, additional periods were found that could not be associated with radial modes. Periods close to the dominant modes were found in a small fraction (4%) of fundamental mode Cepheids but in a significant fraction of objects with exited overtones (e.g. 18% in 1O and 36% in 1O/2O). In 28 first overtone pulsators, additional peaks were found at periods $P_X \approx 0.6 P_{1O}$. Moskalik & Kołaczkowski (2009), who found such peaks already in OGLE-II data, suggested that they are caused by nonradial modes. Histograms in **Figure 3** showing the distribution of double-mode pulsators include the **1O/X** Cepheids.

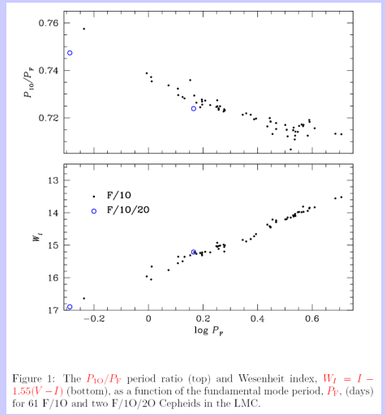

Figure 1: The P_{1O}/P_F period ratio (top) and Wesenheit index, $W_I = I - 1.55(V-I)$ (bottom), as a function of the fundamental mode period, P_F, (days) for 61 F/1O and two F/1O/2O Cepheids in the LMC.

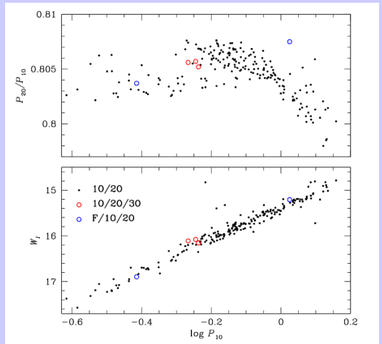

Figure 2: The P_{2O}/P_{1O} period ratio (top) and Wesenheit index (bottom), as a function of the first overtone period, P_{1O}, (days) for 203 1O/2O, two F/1O/2O, and three 1O/2O/3O Cepheids in the LMC. Two **1O/3O Cepheids** occur at $(\log P_{1O}, W_I) = (-0.277, 16.21)$ and $(-0.274, 16.24)$. The period ratio is $P_{3O}/P_{1O} = 0.677$ for both stars.

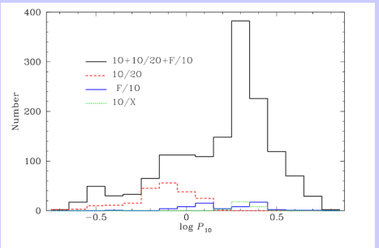

Figure 3: Period distribution for the LMC Cepheids with the first overtone excited. The 1O/2O pulsators constitute 13.8 percent of the sample but dominate in a certain period range. The F/1O pulsators constitute only 4.1 percent. The 1O/X symbol denotes objects (1.9 percent of the sample) with an unidentified modes of periods of about $0.6P_{1O}$. Note that all the 1O/X and the long-period F/1O pulsators occur in the same period range.

Comparison with stellar models

Most of multimode pulsators are found among short-period Cepheids, which, as Alcock et al. (1999) and Alibert et al. (1999) noted, are not well explained in terms of evolutionary models of core-helium burning stars (second and third crossings of the instability strip). Some of them may be in the first crossing phase, which is much faster, but there are also problems with this interpretation.

Data on two periods of radial modes and on Wesenheit indexes, such as shown in **Figures 1 and 2**, yield strong constraints on stellar models. In principle, color data may also be used but they are less accurate. Instead, as a constrain on effective temperatures, a requirement of mode instability was adopted in recent works exploiting data on multimode Cepheids (Moskalik & Dziembowski 2005, Buchler & Szabó 2007, Buchler 2008, Dziembowski & Smolec (2009, hereafter DS)). In the first of these papers, data on the measured periods in two triple-mode Cepheids were used to determine parameters of these objects and the W_I's were used to estimate the distance to LMC. Periods alone on the F/1O Cepheids were used in the second and third papers as a probe of stellar metallicity parameter, Z. In the last paper, which was devoted almost exclusively to the 1O/2O LMC Cepheids, the W_I and period data (**Figure 2**) were used to constrain parameters of these objects, in particular, their masses.

In DS and here, model values of W_I were obtained assuming distance modulus to LMC 18.5 mag (Schaefer 2008). The error of ±0.05 mag translates to ±7 percent uncertainty in stellar mass. Results shown in the plots (**Figures 4 to 6**) were obtained with the OP opacity data (Seaton 2005) calculated for the new solar heavy element mixture (Asplund et al. 2004), using $Z = 0.006$ (most cases) or 0.008. The effects of different choices on models of the F/1O Cepheids were studied by Buchler (2008). We carried linear nonadiabatic calculations of radial modes for deep unfitted envelope models within the relevant temperature range using the code described by Smolec & Moskalik (2008). For luminosity, we first used the values obtained from evolutionary models in the first crossing phase, calculated assuming no overshooting. Then, we considered models with luminosity increments $\Delta \log L = 0.2$ and 0.4 to reproduce the whole range of observed parameters. Models with typical overshooting are brighter by $\Delta \log L \approx 0.15$. Those in the second and third crossings are brighter than models in the first crossing by $\Delta \log L \approx 0.25$ (see Pietrinferni et al. 2004).

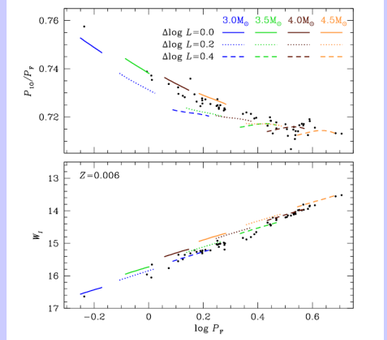

Figure 4: Models of the F/1O Cepheids. The Petersen diagram (top) and PL relations (bottom) for selected models of indicated mass. The segments correspond to the simultaneous instability of the F and 1O modes for models of specified mass and luminosity. Luminosity increments $\Delta \log L$ refer to evolutionary models calculated with $\alpha_{ov} = 0$

In the lower panel of **Figures 4 to 6**, we may see that models of constant mass form nearly a single line in the $\log P - W_I$ plane for specified mode and metallicity. In fact, the dependence on metallicity is quite weak. This means that, once we have credible W_I and the LMC distance, we have quite accurate assessment of a Cepheid mass.

The upper panel of **Figure 4** shows the classical Petersen diagram. We may see that the measured period ratios are well reproduced with our models. Comparing plots in the two panels, we note certain problem for $\log P_F < 0.3$. Models with masses near $3M_\odot$ are in agreement with the observational PL relation if some luminosity excess (presumably due to overshooting) is allowed. Thus, the objects may be understood as first crossers. The calculated period ratio is somewhat low. The agreement would improve by choosing lower Z value (see Buchler 2008). For the F/1O Cepheids with $\log P_F > 0.3$, both the period ratios and the Wesenheit indexes, point to masses near near $4M_\odot$ and the luminosity excess $\Delta \log L \approx 0.4$. These are presumably helium burning objects.

Figures 5 and 6 are from DS, where it was concluded that great majority of the LMC 1O/2O Cepheids have masses $M = 3.0 \pm 0.5 M_\odot$. The objects with $\log P_{1O} \lesssim -0.2$ are well explained with post-main sequence stellar models crossing the instability strip for the first time, calculated assuming no or moderate overshooting. For those with longer periods, which constitute the majority of the sample, a significant luminosity excess is needed. Interpretation in terms of first crossing models requires an overlarge overshooting, perhaps connected with fast rotation. The difficulty of this explanation is the short crossing time of the instability strip while the number of the objects showing the luminosity excess is relatively high. If these are helium burning objects then the difficulty is the low inferred mass. Standard evolutionary track for stars with $M \lesssim 3.5$ and acceptable metallicity do not enter the instability strip in this evolutionary phase.

All five triple-mode Cepheids are most likely first crossing objects. Detailed modeling of two 1O/2O/3O objects implied masses near $3.3M_\odot$. The third one has very similar periods and Wesenheit index (see **Figure 2**), hence, must have a similar mass. Models of similar mass and calculated with moderate overshooting well reproduce data on the two 1O/3O Cepheids. The two F/1O/2O objects occur at very different periods. The one at $\log P_{1O} = -0.4$ has mass $M < 3.0 M_\odot$ and that at $\log P_{1O} = 0.03$ has mass $M \approx 3.5 M_\odot$.

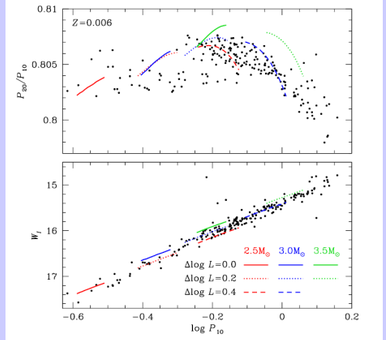

Figure 5: Models of the 1O/2O Cepheids. The Petersen diagram (top) and PL relations (bottom) for selected models of indicated mass. The segments correspond to the simultaneous instability of the 1O and 2O modes for models of specified mass and luminosity. Luminosity increments $\Delta \log L$ refer to evolutionary models calculated with $\alpha_{ov} = 0$.

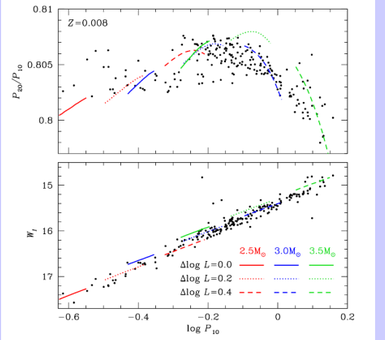

Figure 6: The same as Figure 5 but models were calculated with the metallicity parameter $Z = 0.008$.

Nonradial modes in Cepheids

In the radiative interiors of evolved stars, the Brunt-Väisälä frequency, N, is by orders of magnitude larger than frequencies, ω, of radial modes. This implies that all nonradial modes propagate as high-order gravity waves with radial wave number, k_r, satisfying $r k_r = \sqrt{\ell(\ell+1)} \frac{N}{\omega} \gg 1$. The displacement amplitude is $\xi \propto |C_+ e^{i\Psi} + C_- e^{-i\Psi}| e^{-\lambda t}$ with $\Psi = \int dr k_r$.

Large k_r leads to large radiative losses. Global modes exist as long as $|C_-| \sim |C_+|$, and they are unstable if the driving effects in outer layers are strong enough. However, the wave braking occurring at $k_r|\xi| \approx 1$ may prevent growth of an unstable mode amplitude to observable level (see **Figure 7**). Once it occurs, the reflected wave must be ignored ($|C_-| \approx 0$) and this implies wave energy losses. Only with a resonant energy transfer from a nearby radial mode, detectable amplitude of nonradial modes may be maintained. This mechanism, suggested as an explanations for **peaks close to radial mode frequencies** in RR Lyrae stars (Dziembowski & Mizerski 2004), may apply also to Cepheids.

Strong radiative damping in the interior leads to $|C_-| \ll |C_+|$. This again justifies ignoring the reflected wave. At sufficiently high-ℓ, there are well-trapped modes, which, in spite of the wave losses, remain unstable (Osaki 1977, Dziembowski 1977). Due to cancelation of opposite sign contributions, the net light changes resulting from such mode excitation are expected low.

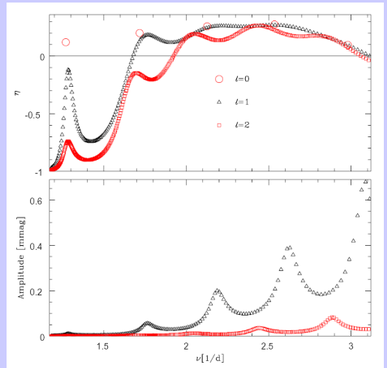

Figure 7: Normalized growth rate $\eta \in [-1, 1]$ (top) and maximum light amplitudes (bottom) for low-ℓ modes in a model of the first crossing Cepheid ($M = 3M_\odot$, $Z = 0.006$, standard overshooting). In this model $\max(N/\omega_F) = 244$. The amplitudes, which were calculated assuming $\max(k_r|\xi|) = 1$, are below detection threshold. There are unstable modes with $\ell \geq 4$, found assuming running wave boundary condition ($|C_-| = 0$).

The troublesome period ratios near 0.6

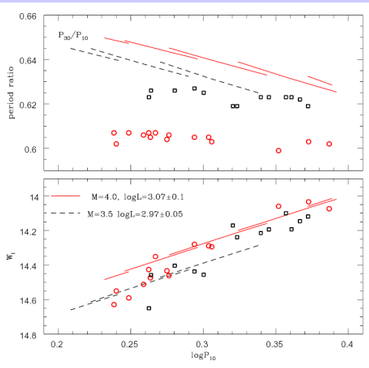

Figure 8: Period ratio (top) and Wesenheit indexes (bottom) for 1O/X Cepheids (symbols) compared with calculated values for the 1O/3O Cepheid models (segments). Unfitted envelope models were calculated for $Z = 0.006$ and temperatures corresponding to the 1O instability range (3O is stable in these models).

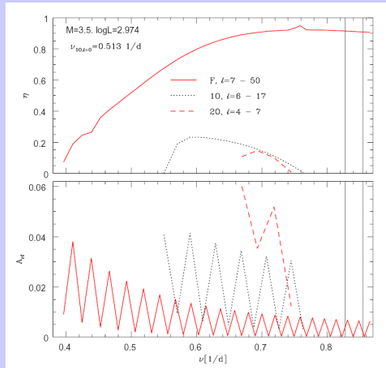

Figure 9: Normalized growth rate η (top) and the amplitude reduction factor, A_{rf} (bottom) for unstable models calculated with the running wave boundary condition for the envelope model of a 1O/X Cepheid ($M = 3.5 M_\odot$, $Z = 0.006$). The A_{rf} factor, which is close to 1 for radial modes, takes into account contribution from local radiative flux changes and surface distortion. Amplitude reduction results from cancelation of opposite sign contributions from various parts of the surface. Two vertical lines correspond to 0.6 and 0.62 period ratios. In these range only the F-modes with ℓ between 46 and 48 are unstable and $A_{rf} \approx 0.007$ for the even-order modes. The measured amplitude ratio of the X to 1O mode is between 0.015 and 0.053.

The challenges

In many cases, models of double-mode Cepheid reproducing observational data disagree with published evolutionary models. The greatest challenge to the stellar evolution theory comes from data on the 1O/2O Cepheids. Most of them are either much too bright for prior-to He-ignition-models or have too low mass ($M \leq 3.5 M_\odot$) for the blue loop to reach the instability strip.

The greatest challenge for stellar pulsation theory is explanation of double-mode pulsators with period ratios near 0.6. Such a period ratio is not expected for any pair of radial modes. It is easy to find a nonradial partners of the first radial overtones fitting the observed ratio but the only unstable modes in the required period range are of very high degrees ($\ell > 40$).

References

Alcock, C. et al. 1999, Ast. Journ., **117**, 920
Alibert, Y., et al. 1999, A&A, **344**, 551
Asplund. M., et al. 2004 A&A, **417**, 751
Buchler, J.R. 2008, ApJ, **680**, 1412
Buchler, J.R. & Szabó, R. 2007, ApJ, **660**, 723
Dziembowski, W.A. 1977, Acta Astr., **27**, 95
Dziembowski, W.A. & Smolec, R. 2009, Acta Astr., **59**, 19
Dziembowski, W.A. & Mizerski, T. 2004, Acta Astr., **54**, 363
Moskalik, P. & Dziembowski, W.A. 2005, A&A, **434**, 1077
Moskalik, P. & Kołaczkowski, Z. 2009, MNRAS, **394**, 1649
Moskalik, P., et al. 2004, ASP Conf. Ser., **310**, 498
Osaki, Y. 1977, Pub. Astr. Soc. Japan, **29**, 235
Pietrinferni, A., et al. 2004, ApJ, **612**, 168
Schaefer, B.E. 2008, Ast. Journ., **135**, 112
Seaton, M. 2005, MNRAS, **362**, L1
Smolec, R. & Moskalik, P. 2008, Acta Astr., **58**, 193
Soszyński, I., et al. 2008a Acta Astr., **58**, 153
Soszyński, I., et al. 2008b Acta Astr., **58**, 163

This work has been supported by the Polish MNiSW Grant No. 1 P03D 011 30